APPLIED GEOPHYSICS, Vol.13, No.1 (March 2016), P. 93-102, 10 Figures.
DOI:10.1007/s11770-016-0544-2

Tomographic inversion of near-surface Q factor by combining surface and cross-hole seismic surveys*

Li Guo-Fa[1], Zheng Hao[♦1], Zhu Wen-Liang[2], Wang Ming-Chao[1], and Zhai Tong-Li[2]

Abstract: The estimation of the quality factor Q plays a fundamental role in enhancing seismic resolution via absorption compensation in the near-surface layer. We present a new geometry that can be used to acquire field data by combining surface and cross-hole surveys to decrease the effect of geophone coupling on Q estimation. In this study, we drilled number of receiver holes around the source hole, each hole has different depth and each geophone is placed geophones into the bottom of each receiver hole to avoid the effect of geophone coupling with the borehole wall on Q estimation in conventional cross-hole seismic surveys. We also propose a novel tomographic inversion of the Q factor without the effect of the source signature, and examine its stability and reliability using synthetic data. We estimate the Q factors of the near-surface layer in two different frequency bands using field data acquired in the Dagang Oilfield. The results show that seismic absorption in the near-surface layer is much greater than that in the subsurface strata. Thus, it is of critical practical importance to enhance the seismic solution by compensating for near-surface absorption. In addition, we derive different Q factors from two frequency bands, which can be treated, to some extent, as evidence of a frequency-dependent Q.
Keywords: near surface, Q factor, tomographic inversion, spectral ratio method, frequency dependence

Introduction

Seismic waves travelling in a viscoelastic medium experience energy attenuation and velocity dispersion (Futterman, 1962), which can be quantified by the quality factor Q. In recent years, experimental research has been carried out in a number of oil fields in China to enhance seismic resolution via absorption compensation in the near surface layer (Shi, et al., 2009; Wang, et al., 2013). Two steps are required in this type of experiment: one is Q estimation, and the other is absorption compensation, with the former having a more fundamental role. The idea of measuring near-surface absorption originated from a near-surface velocity investigation for the purposes of static correction. A near-surface velocity model can be built by identifying the first breaks in uphole seismic data, and then removing the effect of the velocity variation on the seismic reflection time by datum static correction. Because uphole seismic surveys

Manuscript received by the Editor May 8, 2015; revised manuscript received February 22, 2016.
*This research was supported by the National Natural Science Foundation of China (Grant No. 41174117 and 41474109) and the National Key Basic Research Development Program of China (Grant No. 2013CB228606).
1. China University of Petroleum, State Key Laboratory of Petroleum Resource and Prospecting, Beijing 102249, China.
2. Dagang Oilfield, PetroChina, Tianjin 300280, China.
♦Corresponding author: Zheng Hao (Email: zh_geophy@126.com).

have been successfully used in near surface velocity models, it seems straightforward to extend the uphole survey to measure near-surface absorption. Although the two main physical properties, velocity and absorption, can both be estimated from seismic data, their dependences on seismic data are quite different. Velocity estimation is mainly based on the travel times, which is relatively stable with respect to noise and interference. Absorption estimation, on the other hand, makes use of the spectral evolutions of the seismic signal, which are very susceptible to distortion by noise and interference (Li et al., 2012). Hence, the results of the investigation of near-surface absorption by conventional uphole seismic surveys have been somewhat disappointing.

There is a wide variety of methods for estimating Q from seismic data, such as the spectral ratio method (SRM), centroid frequency shift (CFS), risetime and the amplitude decay method (Tonn, 1991). Of these, SRM and CFS are most widely used. The quality factor Q can be estimated using surface seismic surveys (Reine et al., 2012; Lupinacci and Oliveira, 2015), vertical seismic profiles (VSPs) (Hauge, 1981; Zhang et al., 2014), and cross-well seismic surveys (Liao and McMechan, 1997). Brzostowski and McMechan (1992) estimated seismic absorption tomographic inversion by linearly fitting the logarithm of the amplitude spectrum. Quan and Harris (1997) implemented seismic attenuation tomography via the frequency shift method, based on a simple assumption of the wavelet spectrum. Rickett (2006) generalized Q estimation as a linear inversion of the logarithm spectrum, and discussed issues involving regularization. To mitigate the effect of the source radiation pattern on Q estimation, Cao and Zhou (2009, 2010) inverted the Q distribution by using the ratio of the amplitudes of neighboring rays in a shot gather. Cavalca et al. (2011) used tomography to invert the attenuated traveltime (the product of the dissipation factor and travel time), and compensated for seismic absorption in the migrated image. Although a great number of studies have discussed the measurement and estimation of the Q factor using seismic data, few have measured near-surface absorption. Hatherly (1986) measured shallow absorption using seismic refraction data according to the width variation of the seismic pulse with distance. Badri and Mooney (1987) measured the absorption of near-surface unconsolidated sediments, with the sources and receivers all placed at the subsurface; however, the results were unstable. Brzostowski and McMechan (1992) conducted tomographic imaging of near-surface absorption using conventional surface seismic data, but failed to remove the effect of scattering attenuation. Jeng et al. (1999) investigated the frequency dependence of Q in the near-surface layer, and concluded that Q is frequency dependent.

The rest of this paper is organized as follows. First, we propose a new inversion method for near-surface absorption that has no source signature effects, and then we introduce a new geometry for acquiring field data by combining surface and cross-hole surveys, to decrease the effect of geophone coupling in the Q estimation. We use synthetic data to examine the stability and reliability of the proposed method, estimate the near surface absorption using real seismic data acquired in the Dagang Oilfield, and discuss the inversion results in detail.

Theory and method

Estimation of Q via spectral ratio method

Seismic wave propagation in a viscoelastic medium can be expressed by:

$$u(r,f) = s(f)q(r)g(f)\exp\left(-\frac{\pi fr}{Qv}\right), \tag{1}$$

where r is the distance from source to receiver, v is velocity, Q is the quality factor, f is frequency, $s(f)$ is the source signature, $g(f)$ accounts for the receiver coupling response, and $q(r)$ is a frequency-independent term that includes geometrical spread and transmission loss. Taking the logarithm of the ratio of the amplitude spectra in two distances r_2 and r_1, we obtain:

$$\ln\frac{u(r_2,f)}{u(r_1,f)} = \ln\frac{s_2(f)g_2(f)}{s_1(f)g_1(f)} + \ln\frac{q(r_2)}{q(r_1)} - \frac{\pi f(r_2-r_1)}{Qv}. \tag{2}$$

If the source signature and the receiver coupling response are kept invariant, the above equation becomes:

$$d(\Delta t,f) = \ln\left[u(r_2,f)/u(r_1,f)\right] = a - \frac{\pi\Delta t}{Q}f, \tag{3}$$

where $\Delta t = (r_2 - r_1)/v$ and $a = \ln\left[q(r_2)/q(r_1)\right]$ is a frequency-independent constant. We can see that the seismic attenuation $d(\Delta t, f)$ is a linear function with respect to frequency, and the quality factor Q can be estimated from its slope $p = -\pi\Delta t/Q$ by the following:

$$Q = -\frac{\pi\Delta t}{p}. \tag{4}$$

Besides SRM, there are many alternative methods for estimating Q. Tonn (1991) systematically compared different methods, and concluded that no method is superior to others in all cases. Because frequency-independent effects such as geometry spread and transmission loss need not be considered in SRM, it has become the most widely used method for Q estimation.

Tomographic inversion of the near-surface absorption

In this section, we discuss a novel tomographic inversion of the Q factor that has no source signature effect. We assume that seismic waves are fired by n_s shots, and recorded by n_g receivers. The seismic record $x_{ij}(t)$, fired by shot i and recorded by receiver j, can be expressed in the frequency domain as:

$$x_{ij}\left(f\right)=q_{ij}\cdot s_i\left(f\right)\cdot g_j\left(f\right)\cdot \exp\left(\sum_{k=1}^{n_l}-\pi f Q_k^{-1}t_{ijk}\right), \quad (5)$$

where $s_i(f)$ is the signature spectrum of shot i, $g_j(f)$ is the coupling response of geophone j, q_{ij} is a frequency-independent factor accounting for geometric spread and transmission loss, and here, n_l is the layer number, Q_k^{-1} is the inverse Q factor of layer k (also referred to as the dissipation factor), and t_{ijk} is the travel time in layer k. By taking the logarithms, equation (5) becomes:

$$\overline{x}_{ij}\left(f\right)=\overline{q}_{ij}+\overline{s}_i\left(f\right)+\overline{g}_j\left(f\right)-\pi f\sum_{k=1}^{n_l}Q_k^{-1}t_{ijk}, \quad (6)$$

where the overbar denotes the logarithm of the spectrum. To remove the source term $\overline{s}_i\left(f\right)$, we take a certain trace of shot i, e.g., the first trace, as a reference trace, and then subtract its logarithm spectrum from $\overline{x}_{ij}\left(f\right)$, hence:

$$\overline{y}_{ij}\left(f\right)=\overline{b}_{ij}+\overline{g}_j\left(f\right)-\overline{g}_1\left(f\right)-\pi f\sum_{k=1}^{n_l}Q_k^{-1}\Delta t_{ijk}, \quad (7)$$

where $\overline{y}_{ij}\left(f\right)=\overline{x}_{ij}\left(f\right)-\overline{x}_{i1}\left(f\right)$, $\overline{b}_{ij}=\overline{q}_{ij}-\overline{q}_{i1}$, and $\Delta t_{ijk}=t_{ijk}-t_{i1k}$. Assuming that all geophones have the same natural frequency and coupling response, equation (7) can be simplified as:

$$\overline{y}_{ij}\left(f\right)=\overline{b}_{ij}-\pi f\sum_{k=1}^{n_l}Q_k^{-1}\Delta t_{ijk}. \quad (8)$$

The above linear equation system can be written in matrix form as:

$$\begin{vmatrix}\mathbf{y}_1\\ \mathbf{y}_2\\ \vdots\\ \mathbf{y}_{n_a}\end{vmatrix}=\begin{vmatrix}\mathbf{F}_1 & \mathbf{I} & \mathbf{O} & \cdots & \mathbf{O}\\ \mathbf{F}_2 & \mathbf{O} & \mathbf{I} & \cdots & \mathbf{O}\\ \vdots & \vdots & \vdots & \cdots & \vdots\\ \mathbf{F}_{n_a} & \mathbf{O} & \mathbf{O} & \cdots & \mathbf{I}\end{vmatrix}\begin{vmatrix}Q_1^{-1}\\ Q_2^{-1}\\ \vdots\\ Q_{n_l}^{-1}\\ \overline{b}_1\\ \overline{b}_2\\ \vdots\\ \overline{b}_{n_l}\end{vmatrix}, \quad (9)$$

where $n_a=n_s\cdot\left(n_g-1\right)$ is the number of equations, $\mathbf{I}$ is a matrix with all elements being one, $\mathbf{O}$ is a matrix with all elements being zero, $\mathbf{y}_k=\left[y_k\left(f_1\right),y_k\left(f_2\right),\cdots,y_k\left(f_{n_f}\right)\right]^{\mathrm{T}}$ is an attenuation vector comprising $\overline{y}_{ij}\left(f\right)$ and $k=\left(i-1\right)\left(n_g-1\right)+j-1$, sign (T) denotes the transpose, and operator $\mathbf{F}_k$ is the absorption configuration matrix, expressed as:

$$\mathbf{F}_k=\pi\begin{vmatrix}f_1\Delta t_{k,1} & f_1\Delta t_{k,2} & \cdots & f_1\Delta t_{k,n_l}\\ f_2\Delta t_{k,1} & f_2\Delta t_{k,2} & \cdots & f_2\Delta t_{k,n_l}\\ \vdots & \vdots & \vdots & \vdots\\ f_{n_f}\Delta t_{k,1} & f_{n_f}\Delta t_{k,2} & \cdots & f_{n_f}\Delta t_{k,n_l}\end{vmatrix}, \quad (10)$$

where n_f is the frequency number. Equation (9) can be rewritten as:

$$\mathbf{y}=\mathbf{Fm}. \quad (11)$$

The model vector $\mathbf{m}$ can be obtained by minimizing the objective function as follows:

$$e=\left(\mathbf{y}-\mathbf{Fm}\right)^{\mathrm{T}}\mathbf{W}^2\left(\mathbf{y}-\mathbf{Fm}\right)+\mathbf{m}^{\mathrm{T}}\mathbf{D}^{\mathrm{T}}\mathbf{Dm}, \quad (12)$$

where the diagonal weighting matrix $\mathbf{W}$ emphasizes the contribution to the model space, and is usually chosen to be proportional to the travel time difference, and the constraint operator $\mathbf{D}$ controls the tradeoff between stability and accuracy.

Choice of geometry

To estimate the reliable near-surface Q factor, the geometries used should satisfy the following requirements to the degree possible: (1) the direct waves used for the absorption estimation should avoid noise and interference effects; (2) the source signature should be invariant, or else its effect should be removed in the Q estimation; (3) the receiver coupling response should be invariant, or else its effect should be removed in the Q estimation; and (4) project costs should be minimized, which is typically neglected in academic research but is an essential consideration in real seismic surveys.

The surface seismic survey, the most widely used method for field data acquisition, is not suitable for Q measurement because of the associated wavefield interference and noise disturbance. The uphole survey is commonly used in the near-surface velocity model, and seems preferable to Q estimation because of the simplicity of the wavefields. The uphole survey can be implemented by drilling a borehole from the ground surface to a level deep enough to sample all relevant near-surface layers, then the sources are fired at various depths from deep to shallow, and the direct waves are recorded by geophones at the ground surface. Once the data have been acquired, the times from the source to the receiver are measured and adjusted with a geometric correction to generate vertical times, based on a determination of which velocity and thickness measurements of the near-surface layers can be calculated out. In theory, it would seem that the uphole survey, as a small-scale VSP survey (Blias, 2012), could be conveniently extended to measure the near-surface absorption. In practice, however, its application usually fails because of the source signature variation with depth. Figure 1 shows two direct waves and their spectra, acquired by an uphole survey in the Dagang Oilfield. One was fired at a depth of 9 m and the other at a depth of 15 m. Although the 15-m direct wave experienced more absorption when it arrived at the surface geophone, its peak frequency of 117 Hz was still 41 Hz higher than that of the 9-m direct wave. If we directly estimate Q from the spectral ratio without considering the effect of the source signature, we obtain a negative Q factor, which is contradictory to the physical nature of seismic absorption.

There is another type of seismic survey, sometimes called the downhole seismic survey, whereby seismic waves are fired at or close to the surface, and recorded at different depths in the borehole. The source effect on the Q estimation can be successfully avoided because all the seismic signals have the same source signature. However, it is difficult, and even impossible, to ensure that all the geophones that are tightly coupled with the unconsolidated borehole wall will have the same coupling responses. The cross-hole survey has been considered to be the optimal geometry for Q measurement, in which two holes are drilled—one for the source and the other for the receiver. However, this type of survey has the same problem as that of the downhole survey, which is the difficulty of geophone coupling with the borehole wall.

We have developed a novel seismic acquisition geometry for measuring near-surface absorption by combining the surface and cross-hole surveys. As shown in Figure 2, a source borehole is drilled, and a 2D seismic line is arranged near the hole. Then, a number of receiver holes are drilled around the source hole to different depths. Geophones are then placed at the bottom of each receiver hole, instead of at different depths in the same hole. In this way, we avoid the difficulty of geophone coupling with the borehole wall.

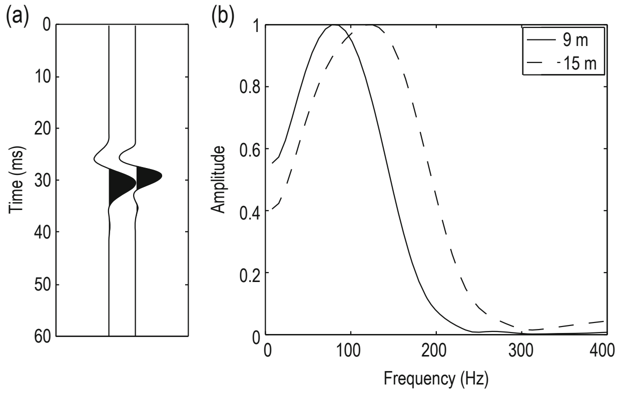

Fig.1 Two direct waves (a) fired at the depths of 9 m (left) and 15 m (right), as well as their Fourier spectra (b).

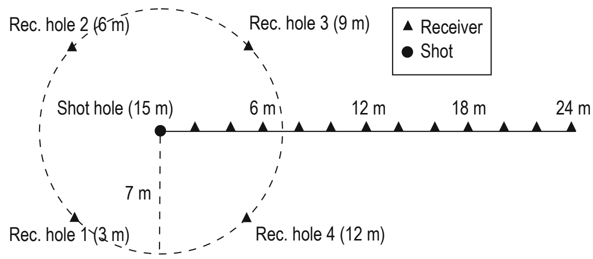

Fig.2 Geometry used to measure the near-surface absorption by combining surface and cross-hole surveys.

Synthetic tests

As shown in Figure 3, we assumed that the near surface consisted of two layers—weathering and sub-weathering layers. The thickness of the weathering layer was 4 m, and its velocity and quality factor were $v_1 = 450$ m/s and $Q_1 = 2.0$, respectively. The velocity and quality factor of the sub-weathering layer were $v_2 = 1300$ m/s and $Q_2 = 10.0$, respectively. The depth of the source hole was 15 m. The shots were fired at depths from 15 m to 8 m with intervals of 1 m. The depth of the receiver hole was 12 m, and its lateral distance from the source hole was 7 m. Four geophones were placed in the receiver hole at the depths of 3, 6, 9, and 12 m, respectively. Meanwhile, 12 geophones were placed on the ground in a line at 2-m intervals, and the minimum and the maximum offsets from the source hole were 2 and 24 m, respectively. We simulated the source signature by a Ricker wavelet with a 90° phase, and to account for the signature variation, we set its peak frequency to be a random integer between 300 to 400 Hz.

Seismic wave propagation in a viscoelastic medium can be expressed in the $f-k$ domain as follows (Li et al., 2015a):

$$p(z,k_x,f)=p(z_0,k_x,f)\exp\left(-i(z-z_0)\sqrt{k^2-k_x^2}\right), \quad (13)$$

where z is depth, f is frequency, k_x is the horizontal wavenumber, and p is the wavefield initialized by the source signature when $z = z_0$. To introduce seismic absorption, the wavenumber k should be taken as a complex value, expressed by:

$$k = k_r + jk_i = \frac{2\pi f}{v(f)} + j\frac{\pi f}{Qv(f)}, \quad (14)$$

where j is an imaginary unit, the real part k_r and the imaginary part k_i account for velocity dispersion and energy attenuation, respectively, and $v(f)$ is frequency-dependent velocity, expressed as:

$$v(f)=v(f_0)\left[1+\frac{1}{\pi Q}\ln\frac{f}{f_0}\right], \quad (15)$$

where f_0 is the reference frequency. We set f_0 = 300 Hz in this experiment.

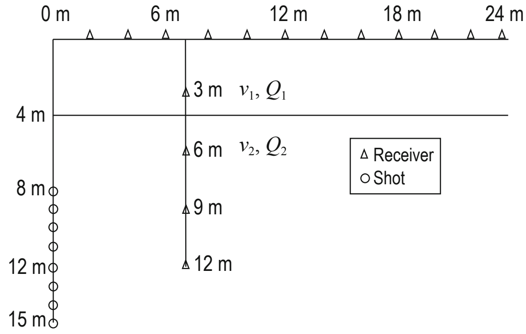

Fig.3 Cross-hole geometry combined with surface survey for the synthetic test.

Using the geometry shown in Figure 3, we simulated eight shot gathers. In two of them, one fired at depths of 8 m with a peak frequency of 300 Hz and the other fired at depths of 15 m with a peak frequency of 380 Hz, as shown in Figure 4. In the shot gathers, we recorded channels 1 to 12 on the ground surface, and recorded channels 13 to 16 in the receiver hole. Neglecting the effect of geophone coupling, the accuracy and stability of the absorption inversion were mainly affected by noise disturbance and velocity error. Figure 5a shows the results of the Q inversion when the signal-to-noise ratios (SNR) are 50 and 10, respectively. When the SNR = 50, the inverted Qs for the weathering and sub-weathering layers are 2.01 and 10.36, with relative errors of 0.31% and 3.55%, respectively. When the SNR = 10, the inverted Qs for the two layers are 2.12 and 9.20, with relative errors of 6.0% and 8.0%, respectively. We can see that the proposed method is stable with respect to noise, as it makes full use of the direct waves recorded both on the ground surface and in the receiver borehole. Figure 5b shows the inverted Qs when we used velocities with ±10% error. When we used velocities with

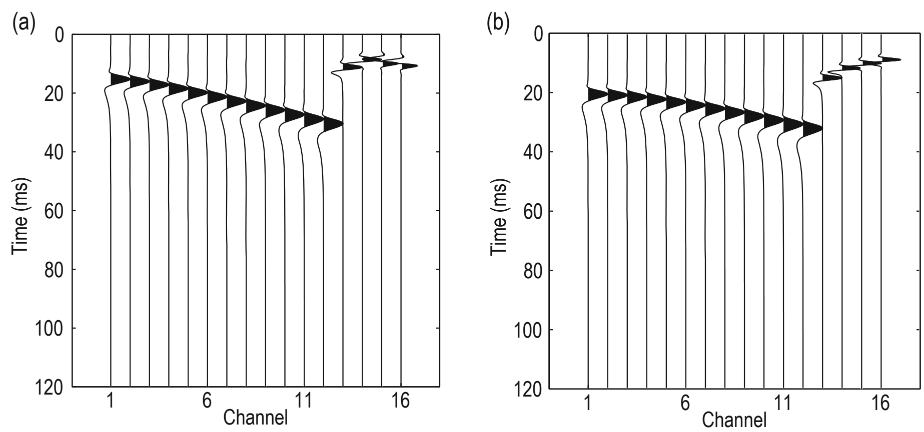

Fig.4 Two shot gathers fired at 8 m (a) and 15 m (b). The peak frequencies of the source signatures for the two shots are 300 Hz and 380 Hz, respectively.

±10% error, the inverted Qs for the weathering and sub-weathering layers are 1.82 and 9.09, and their relative errors are –9.0% and –9.1%, respectively. When we use velocities with –10% error, the inverted Qs for the two layers are 2.22 and 11.11, and their relative errors are 11.0% and 11.1%, respectively. In an uphole seismic survey, because it is not difficult to control the velocity error to within 10%, the effect of the velocity error on the Q estimation is acceptable.

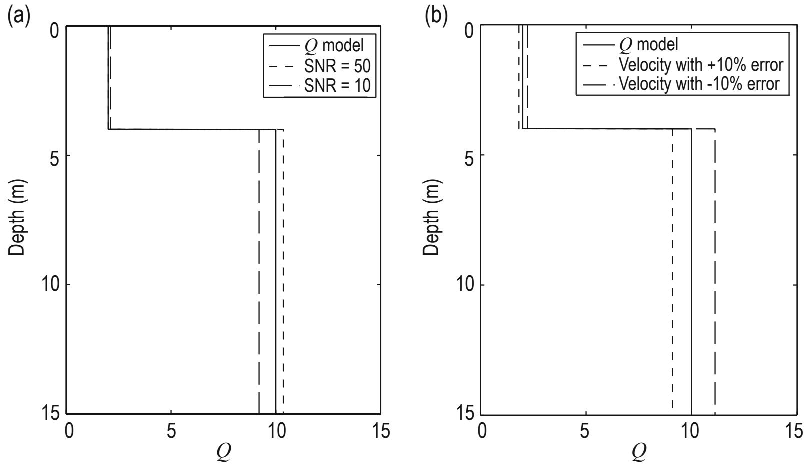

Fig.5 Effects of noise disturbance (a) and velocity error (b) on Q inversion.

Application to field data

The experimental site is located in the Gangdong area of the western Dagang Oilfield, where the ground surface is flat, and the near-surface structure consists of only two layers-the weathering and sub-weathering layers. The thickness of the weathering layer is around 4 m, and that of the sub-weathering layer is more than 40 m. We used the geometry shown in Figure 3 to acquire the field data. A total 15 shots were fired at depths from 15 m to 1 m, with intervals of 1 m. To decrease the effect of geophone coupling on the Q estimation, in addition to using geophones with the same natural frequency, we carefully examined the geophones to be used to guarantee that they had the same receiving response. To avoid the difficulties associated with placing all the geophones tightly coupled with the borehole wall, as shown in Figure 2, we drilled four receiver holes, with equal offsets of 7 m, but different azimuths, from the source hole, to depths of 3, 6, 9, and 12 m, respectively, and placed the geophones at the bottom of each receiver hole to ensure that the coupling responses were as identical as possible. We established the velocity model by selecting the first break times and transferring them to velocity. As shown in Figure 6, the near surface consists of the weathering and sub-weathering layers. The thickness of the weathering layer is 4 m, and the velocity increases to 1592 m/s in the sub-weathering layer from 542 m/s in the weathering layer. As we can see from the distribution of the selected first breaks, the velocity is almost invariant within the weathering and sub-weathering layers, which implies that because of the weak scattering effect the effect of scattering attenuation on the Q estimation can be neglected.

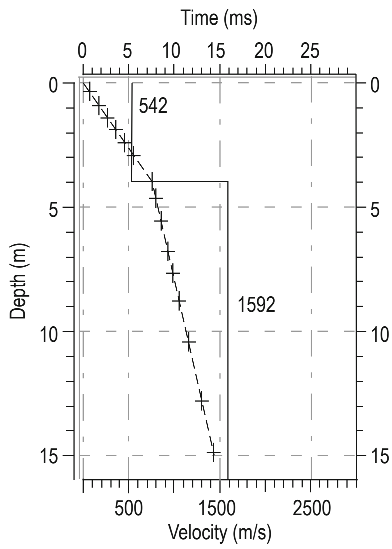

Fig.6 Near-surface velocity model established using the first breaks.

It is crucial in Q estimation to precisely extract direct waves because they are usually contaminated by noise and interference from other wavefields. Figure 7 shows four shot gathers fired at different depths. We can see that the direct waves were strongly contaminated by ground rolls. Although the strength of the ground rolls decreased gradually with increasing source depth, the seven traces with offsets greater than 10 m remained immersed in the ground rolls even when the source depth was only 8 m. We attempted to remove the ground rolls by $f - k$ filtering, however, the results were not satisfactory. Rather than being perfectly linear, a ground roll is usually pseudo-linear, with behavior somewhere between linear and random noise, because of velocity dispersion being an inherent characteristic. It is difficult to remove this kind of pseudo-linear noise by regular noise attenuation methods. In addition, the multi-channel filter used to suppress ground rolls tends to blur the spectral difference between direct waves, which consequently leads to a Q estimation with low accuracy. Therefore, we excluded all traces contaminated by ground rolls to ensure the reliability of the Q estimation.

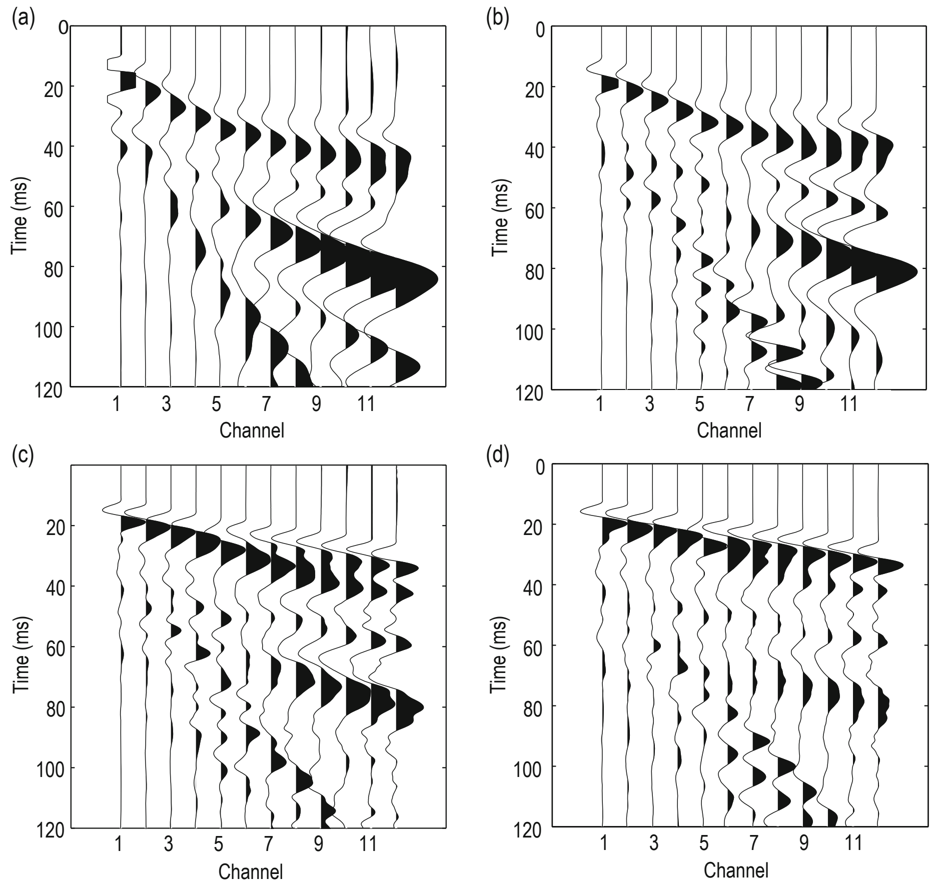

Fig.7 Four shot gathers received on the ground surface, fired at depths of 2 m (a), 4 m (b), 6 m (c), and 8 m (d).

Figure 8 shows two shot gathers fired at depths of 9 m and 13 m, respectively. There were 16 channels in each shot gather, for which channels 1 to 12 were recorded on the ground surface, and channels 13 to 16 were recorded in the receiver holes. When the source depth reached 9 m, the ground rolls disappeared, and direct waves could be clearly recognized in the shot gathers. We can see from Figure 8 that channel 5 was not well coupled with the ground, thus, we discarded it from the Q estimation. We extracted the direct waves by windowing the seismic records using a Hanning window of 24 ms, centered at the peak of the direct wave. To avoid the effect of the near field on the Q estimation (Mangriotis et al., 2011), we set the minimum frequency used for absorption inversion as 100 Hz. In the meantime, to prevent high frequency noise, we set the maximum frequency as 270 Hz. Using the aforementioned method, we inverted the Q factors using two frequency bands of 100−200 Hz and 170−270 Hz. From the inversion results shown in Figure 9, we can see that the Q values for the weathering and sub-weathering layers are around 3.0 and 12.0, respectively. The Q values of the subsurface strata are commonly greater than 30 (Sams et al., 1997), much larger than those of the near-surface layers. Seismic waves are strongly absorbed and attenuated when travelling through the near-surface layer, therefore, it is of great practical significance to enhance the seismic resolution by compensating for near-surface absorption. We also note that the inversion results are somewhat different between the two frequency bands; the Q values for the weathering and sub-weathering layers were 3.3 and 12.5, respectively, when we used a frequency band of 100−200 Hz, whereas they were 2.8 and 11.0, respectively, when we changed the frequency band to 170−270 Hz. To some extent, this difference suggests that Q is dependent on frequency. Next, we discuss this issue in detail.

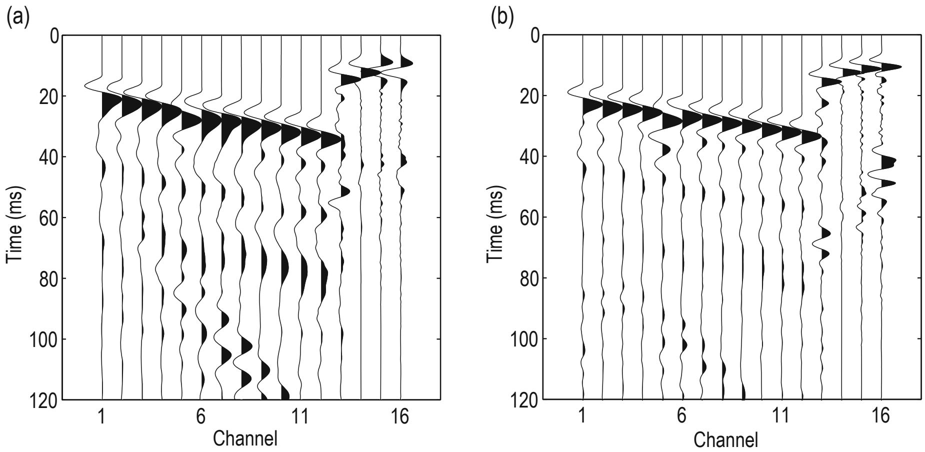

Fig.8 Two shot gathers fired at depths of 9 m (a) and 13 m (b).

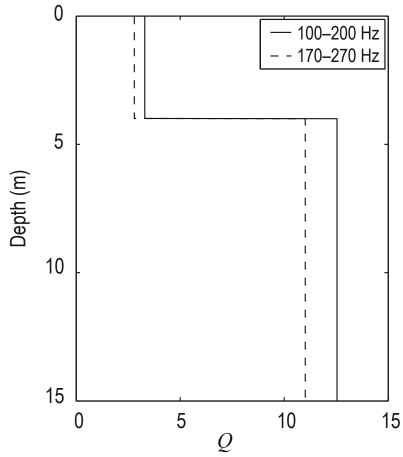

Fig.9 Near-surface Q factors estimated using frequency bands of 100−200 Hz (solid) and 170-270 Hz (dotted).

Although the assumption of a constant Q is widely used in seismic exploration, results from the absorption mechanism of wave-induced fluid flow (Müller et al., 2010) and laboratory measurements of samples (Wang et al., 2012; Piane et al., 2014) tend to suggest that the Q factor, in fact, depends on frequency. Kan et al. (1983) claimed to have observed a frequency-dependent Q in a spectral analysis of VSP data. Li et al. (2015b) also attempted to estimate a frequency-dependent Q from real seismic data. However, in-situ evidence of frequency-dependent Qs from seismic surveys is still lacking. Jones (1986) attributed the lack of in-situ evidence to the difficulty of making appropriate seismic measurements and to the narrow bandwidth of seismic data acquired in the field. Lots of evidence for frequency-dependent Qs has been provided from oceanic measurements using a sonar source (Carey et al. 2008), in which the simulated results well matched those of real measurement only when using a frequency-dependent Q (Zhou et al., 2009). A frequency-dependent Q can usually be expressed as follows (Gurevich and Pevzner, 2015):

$$Q^{-1}(f) = Q^{-1}(f_0)\left(\frac{f}{f_0}\right)^{\gamma}, \tag{16}$$

where f_0 is the reference frequency, and the exponent γ is a constant, with a usual value in the range $-1.0 < \gamma < 1.0$. If we substitute equation (16) into equation (3), seismic attenuation with frequency can be rewritten as:

$$d(\Delta t, f) = c - \frac{\pi Q^{-1}(f_0)\Delta t}{f_0^{\gamma}} f^{1+\gamma}. \tag{17}$$

We can see that seismic attenuation with frequency becomes nonlinear. The Q factor, estimated by linearly fitting to the seismic attenuation, will depend on the frequency band used. Figure 10 shows the attenuation function within the frequency band 100−270 Hz, when

f_0 = 350 Hz, $Q_0^{-1}(f_0)$ = 0.05, γ = 0.6, and Δt = 100 ms. Seismic attenuation is not a straight line, because of the frequency dependence of the Q factor. Fitted straight lines and estimated Qs, using the two frequency bands 100−185 Hz and 185−270 Hz, are also shown in Figure 10. We derived different Q values from the two frequency bands with Q = 21.56 for the first band and Q = 16.24 for the second band.

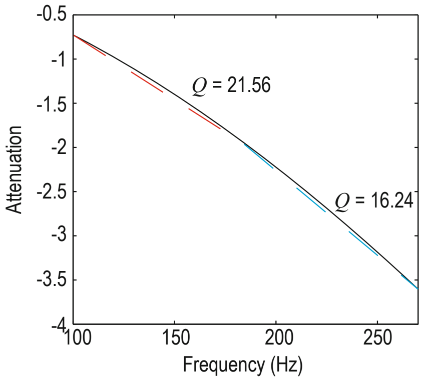

Fig.10 For a frequency-dependent *Q*, seismic attenuation becomes nonlinear with respect to frequency.

Conclusions

We proposed a novel method of data acquisition and tomographic inversion, by combining surface and cross-hole surveys, for measuring near-surface absorption. First, we decreased the effect of receiver coupling on Q estimation using the proposed geometry, then remove the effect of the source signature on the Q inversion by choosing a reference trace in the shot gather. Integrating surface and cross-hole survey data in the inversion scheme yields a stable solution in the presence of noise disturbance. The inversion results from the field data suggest that the dissipation factors of the near-surface layer are much greater than those of the subsurface strata, and seismic waves undergo strong absorption and attenuation when travelling through the near-surface layer. Therefore, it is of great practical significance to enhance seismic resolution by compensating for near-surface absorption. The mechanism of the seismic absorption suggests a frequency-dependent Q and nonlinear seismic attenuation. We estimated the Q factors of the near-surface layer using tomographic inversion, and observed their differences in two frequency bands, which can be treated, to some extent, as evidence of a frequency-dependent Q.

Acknowledgements

We are grateful to Mingqiang Cao and Xiaoming Zhang for their helpful discussion.

References

Badri, M., and Mooney, H. M., 1987, Q measurements from compressional seismic waves in unconsolidated sediments: Geophysics, **52**(6), 772−784.

Blias, E., 2012, Accurate interval Q-factor estimation from VSP data: Geophysics, **77**(3), WA149–WA156.

Brzostowski, M. A., and McMechan, G. A., 1992, 3-D tomographic imaging of near-surface seismic velocity and attenuation: Geophysics, **57**(3), 396−403.

Cao, H., and Zhou, H., 2009, Reflection attenuation tomography: comparison between two neighboring ray approaches: 79th Annual International Meeting, SEG, Expanded Abstracts, 4009−4013.

Cao, H., and Zhou, H., 2010, Reflection attenuation tomography: a field example: 80th Annual International Meeting, SEG, Expanded Abstracts, 2815−2819.

Carey, W. M., Pierce, A. D., Evans, R. E., and Holmes, J. D., 2008. On the exponent in the power law for the attenuation at low frequencies in sandy sediments: Journal of the Acoustical Society of America, **124**(5), EL271−EL277.

Cavalca, M., Moore, I., and Zhang, L., 2011, Ray-based tomography for Q estimation and Q compensation in complex media: 81th Annual International Meeting, SEG, Expanded Abstracts, 3989−3993.

Futterman, W. I., 1962, Dispersive body waves: Journal of Geophysical Research, **67**(13), 5279−5291.

Gurevich, B., and Pevzner, R., 2015. How frequency dependency of Q affects spectral ratio estimates: Geophysics, **80**(2), A39−A44.

Hatherly, P. J., 1986, Attenuation measurements on shallow seismic refraction data: Geophysics, **51**(2), 250−254.

Hauge, P. S., 1981, Measurements of attenuation from vertical seismic profiles: Geophysics, **46**(11), 1548-1558.

Jeng, Y., Tsai, J. Y., and Chen, S. H., 1999, An improved method of determining near-surface Q: Geophysics, 64(5), 1608−1617.

Jones, T. D., 1986. Pore fluids and frequency dependent wave propagation in rocks: Geophysics, 51(10), 1939–1953.

Kan, T. K., Batzle, M. L., and Gaiser, J. E., 1983. Attenuation measured from VSP: evidence of frequency-dependent Q: 53th Annual International Meeting, SEG,

Expanded Abstracts, 589−590.
Li, G., Peng, G., Yue, Y., Wang W., and Cui, Y., 2012, Signal-purity-spectrum-based colored deconvolution: Applied Geophysics, **9**(3), 333–340.
Li, G., Liu, Y., Zheng, H., and Huang, W., 2015a, Absorption decomposition and compensation via a two-step scheme: Geophysics, **80**(6), V145−V155.
Li, G., Zheng, H., Zhang, X., Lin, X., and Cao, M., 2015b, Frequency-dependent near-surface Q factor measurements via a cross-hole survey: Journal of Applied Geophysics, **121**, 1–12.
Liao, Q., and McMechan, G. A., 1997, Tomographic imaging of velocity and Q, with application to crosswell seismic data from the Gypsy Pilot Site, Oklahoma: Geophysics, **62**(6), 1804–1811.
Lupinacci, W. M., and Oliveira, S. A. M., 2015, Q factor estimation from the amplitude spectrum of the time–frequency transform of stacked reflection seismic data: Journal of Applied Geophysics, **114**, 202−209.
Mangriotis, M. D., Rector, J. W., and Herkenhoff, E. F., 2011, Effects of the near-field on shallow seismic studies: Geophysics, **76**(1), B9−B18.
Müller, T. M., Gurevich, B., and Lebedev, M., 2010, Seismic wave attenuation and dispersion resulting from wave-induced flow in porous rocks—A review: Geophysics, **75**(5), A147−A164.
Piane, C. D., Sarout, J., Madonna, C., Saenger, E. H., Dewhurst, D. N., and Raven, M., 2014, Frequency-dependent seismic attenuation in shales: experimental results and theoretical analysis: Geophysical Journal International, **198**(1), 504−515.
Quan, Y., and Harris, J. M., 1997, Seismic attenuation tomography using the frequency shift method: Geophysics, **62**(3), 895–905.
Reine, C., Clark, R., and Van der Baan, M., 2012, Robust prestack Q-determination using surface seismic data: Part 2–3D case study: Geophysics, **77**(1), B1−B10.
Rickett, J., 2006, Integrated estimation of interval-attenuation profiles: Geophysics, **71**(4), A19−A23.
Sams, M. S., Neep, J. P., Worthington, M. H., and King, M. S., 1997, The measurement of velocity Dispersion and frequency-dependent intrinsic attenuation in sedimentary rocks: Geophysics, **62**(5), 1456−1464.
Shi, Z., Tian, G., Wang, B., and Chen, S., 2009, Near-surface absorption compensation technology and its application in the Daqing: Applied Geophysics, **6**(2), 184−191.
Tonn, R., 1991, The determination of the seismic quality factors Q from VSP data: A comparison of different computational methods: Geophysical Prospecting, **39**(1), 1−27.
Wang, C., Pei, J., and Wang, J., 2013, Near-surface Q model building and inverse Q filtering：A case study from Daqing oilfield, China: 83th Annual International Meeting, SEG, Expanded Abstracts, 1821−1825.
Wang, S., Zhao, J., Li, Z., Harris, J. M., and Quan, Y., 2012, Differential Acoustic Resonance Spectroscopy for the acoustic measurement of small and irregular samples in the low frequency range: Journal of Geophysical Research, **117**, B06203.
Zhang, G. L., Wang, X. M., He, Z. H., Cao J. X., Li, K. E., and Rong, J. J., 2014, Interval Q inversion based on zero-offset VSP data and applications: Applied Geophysics, **11**(2), 235−244.
Zhou, J. X., Zhang, X. Z,. and Knobles, D. P., 2009. Low-frequency geoacoustic model for the effective properties of sandy sea bottoms: Journal of the Acoustical Society of America, **125**(5), 2847−2866.

Li Guo-Fa: See biography and photo in the **Applied Geophysics** September 2012 issue, P. 340